Continuous-time discrete-space models of marine mammal exposure to Navy sonar

Charlotte M. Jones-Todd[a,1,*], Enrico Pirotta[b,c,1,*], John W. Durban[d], Diane E. Claridge[e], Robin W. Baird[f], Erin A. Falcone[g], Gregory S. Schorr[g], Stephanie Watwood[h], Len Thomas[i]

[a]*Department of Statistics, University of Auckland, Auckland, 1142, New Zealand*
[b]*Department of Mathematics and Statistics, Washington State University, 14204 NE Salmon Creek Avenue, Vancouver, WA 98686, United States of America*
[c]*School of Biological, Earth and Environmental Sciences, University College Cork, Distillery Fields, North Mall, Cork T23 N73K, Ireland*
[d]*SEA, Inc., 9099 Soquel Drive, Suite 8, Aptos, CA 95003, United States of America*
[e]*Bahamas Marine Mammal Research Organization, Marsh Harbour, Abaco, Bahamas*
[f]*Cascadia Research Collective, Olympia, WA 98501, United States of America*
[g]*Marine Ecology and Telemetry Research, 2420 Nellita Rd NW, Seabeck, WA 98380, United States of America*
[h]*Naval Undersea Warfare Center Division, Code 74, Newport, RI 02840, United States of America*
[i]*Centre for Research into Ecological and Environmental Modelling, The Observatory, University of St Andrews, KY16 9LZ, Scotland*

[*]Corresponding authors: Charlotte M Jones-Todd, c.jonestodd@auckland.ac.nz; Enrico Pirotta, enrico.pirotta@wsu.edu

[1]*Authors contributed equally to this manuscript.*

Abstract

1. Assessing the patterns of wildlife attendance to specific areas is relevant across many fundamental and applied ecological studies, particularly when animals are at risk of being exposed to stressors within or outside the boundaries of those areas. Marine mammals are increasingly being exposed to human activities that may cause behavioural and physiological changes, including military exercises using active sonars. Assessment of the population-level consequences of anthropogenic disturbance requires robust and efficient tools to quantify the levels of aggregate exposure for individuals in a population over biologically relevant time frames.

2. We propose a discrete-space, continuous-time approach to estimate individual transition rates across the boundaries of an area of interest, informed by telemetry data collected with uncertainty. The approach allows inferring the effect of stressors on transition rates, the progressive return to baseline movement patterns, and any difference among individuals.

3. We apply the modelling framework to telemetry data from Blainville's beaked whale (*Mesoplodon densirostris*) tagged in the Bahamas at the Atlantic Undersea Test and Evaluation Center (AUTEC), an area used by the US Navy for fleet readiness training.

4. We show that transition rates changed as a result of exposure to sonar exercises on the range, reflecting an avoidance response.

5. *Synthesis and applications.* Our approach will support the assessment of the aggregate exposure of individuals to sonar and the resulting

population-level consequences, a legal requirement for the US Navy on their ranges. The approach has potential applications across many applied and fundamental problems where telemetry data are used to characterise animal occurrence within specific areas.

Keywords: Aggregate exposure, area attendance, beaked whales, individual-level random effects, sonar disturbance, Template Model Builder, transition probability

1. Introduction

As a result of the expansion of human activities, individuals from wildlife populations are increasingly being exposed to a variety of anthropogenic stimuli (Halpern et al., 2008; Sanderson et al., 2002; Díaz et al., 2019). Some human activities can have non-lethal effects on exposed individuals, causing deviations in their natural patterns of behavior and physiology (Pirotta et al., 2018a; Frid and Dill, 2002). Current European Union (European Habitats Directive 92/43/EEC) and United States (Endangered Species Act, 16 U.S.C. §§ 1531 et seq.; Marine Mammal Protection Act, 16 U.S.C. §§ 1361 et seq.) legislation mandates an assessment of the population-level consequences of these behavioral and physiological changes. Understanding where, when, and how often animals come into contact with human activities is the first step towards this assessment. In particular, quantifying population consequences requires an evaluation of 1) the proportion of the population that is exposed and 2) the aggregate exposure of each individual (i.e., the total duration and intensity of exposure to the stressor of interest during a biologically-meaningful period (Pirotta et al., 2018a)). Various factors influence the patterns of exposure of individuals in space and time. For example, a population's movement patterns, the size of individual home ranges and the motivation underlying the use of the area of interest (e.g., whether the area contains foraging patches or is used solely for transit) will all contribute to determine if each individual in a population is exposed at all and, if so, its aggregate exposure, e.g. (Pirotta et al., 2018b; Jones et al., 2017; Merchant

et al., 2018).

Many marine organisms rely on the use of sound for important life-history functions (e.g., communication and prey finding) (Montgomery and Radford, 2017). In recent decades, extensive work on the population consequences of disturbance has thus been motivated by growing concerns on the effects of increasing anthropogenic noise pollution in the ocean (Popper and Hawkins, 2016), particularly on marine mammals (National Research Council, 2005; Nowacek et al., 2007). Among the various sources of noise, cetacean populations may be affected by military operations using active sonar (Southall et al., 2016). Dedicated experiments and opportunistic exposure studies have shown that animals can respond to active sonars by changing their horizontal movement and diving behavior, leading to interruption of foraging activity, habitat displacement and, potentially, changes in their physiology (Tyack et al., 2011; Southall et al., 2016; Falcone et al., 2017; Harris et al., 2018; Joyce et al., 2019). As such, current environmental impact statements conducted on navy ranges require an assessment of the number of individuals that respond to sonar exercises; this number can be estimated from the probability of an individual getting exposed to the noise source, and the probability of responding when exposed to a certain noise level (i.e, the dose-response curve) (Harris et al., 2018).

A suite of individual-based animal movement models has been developed to estimate the number of individuals that are exposed and respond over the duration of a single navy exercise, e.g., (Frankel et al., 2002; Donovan

et al., 2017; Houser, 2006; U.S. Department of the Navy, 2018). However, these models are not suitable for the estimation of individuals' exposure to sonar over time and across multiple exercises, because their predictions become increasingly unrealistic when simulating movements for more than a few days, with individuals tending to drift away from the range area (Donovan et al., 2017). Moreover, simulating fine-scale animal movements over a long time period is computationally intensive, and unnecessary when the animals are outside the area of interest. To overcome these difficulties, most existing models treat each day as separate and do not tally the number of times individuals are exposed over longer periods, even though predictions of population-level effects will change drastically depending on the level of aggregate exposure (Donovan et al., 2017; Pirotta et al., 2018a). An alternative method is required to characterize the long-term patterns of individual occurrence in the target area and the effect of exposure and response to disturbance on these patterns. Such a method would then form the basis for a detailed quantification of the number of times each individual is exposed when inside the area and thus susceptible to respond to disturbance. In order to capture the various aspects of the ecology of a population that could influence usage of the area, the method should be informed using empirical movement data collected from individuals in the population over a comparable time scale. Modern satellite telemetry technologies allow us to track marine mammal movements for long periods, and could therefore be used to characterize the attendance to specific areas of interest. However, they are

often associated with substantial spatial error in animal relocations (Costa et al., 2010; McClintock et al., 2015).

In this study, we develop a discrete-space, continuous-time analytical approach to monitor the occurrence of animals in an area of interest and their transition rates across the boundaries of that area, informed by telemetry data collected with uncertainty. Our goal is to be able to estimate the aggregate exposure and response to sonar of individuals in a population over biologically relevant time periods (e.g., one year). The approach allows for differences in movement patterns among individuals. Importantly, the potential repulsive effect that the activity under analysis has on the animals and the progressive decay of such effect over time can also be quantified (Tyack et al., 2011; Moretti et al., 2014). While the approach is motivated by and applied to case studies involving the exposure of cetaceans to disturbance from active sonar operations on US Navy ranges, it is widely applicable to other contexts and types of stressors. The method would also be useful in situations where the estimation of the movements in and out of an area is of interest, irrespective of the presence of anthropogenic stressors (e.g., to monitor the attendance of individuals to a protected area).

2. Materials and Methods

2.1. Telemetry data and exposure information

We use satellite telemetry data from seven Blainville's beaked whales (*Mesoplodon densirostris*) tagged between 2009 and 2015 within or near the

Atlantic Undersea Test and Evaluation Center (AUTEC), in the Bahamas (broadly referred to as 'range', see Fig. 1). This region is regularly used by the US Navy to carry out military exercises with active sonar. Tagging was carried out in advance of large-scale exercises (Submarine Command Courses) to monitor resulting changes in the animals' movement behaviour.

Data collection techniques are described in detail in Joyce et al. (2019). Animals were instrumented with Wildlife Computers SPLASH transmitters ($n = 2$, Mk-10; Wildlife Computers Inc., Redmond, WA, USA) and SPOT model tags ($n = 5$, AM-S240A-C; Wildlife Computers Inc.) in the Low Impact Minimally Percutaneous External-electronics Transmitter (LIMPET) configuration, see Table A.1 in Appendix A. Tags were attached on or near the dorsal fin from distances of 5-25 m using a crossbow or black powder gun (Joyce et al., 2019; Tyack et al., 2011). Location estimates of tagged whales were provided by the Argos system based on the Kalman filtering method (Lopez et al., 2013).

Information on the use of mid-frequency active sonars (MFAS) at AUTEC was available from records in the US Navy's internal Sonar Positional Reporting System (SPORTS) database (including, but not limited to, the Submarine Command Courses analysed in Joyce et al. (2019)). While SPORTS data are known to suffer from transcription errors and incomplete records, they offered the best available source of sonar information. Specifically, we extracted bouts of high-power and mid-power MFAS use (*sensu* Falcone et al. (2017)) during tag deployment periods, and calculated the number of days

since exposure to a sonar event for each individual relocation. The outline of the hydrophone array at AUTEC was used as the range boundary, and animals were considered exposed when occurring within this area during sonar activity.

In addition to tracks of *M. densirostris* from AUTEC, we applied our modelling approach to four other cetacean species with varying movement behavior and ecology, occurring over two different US Navy ranges, the Hawaii Range Complex (HRC) and the Southern California Range Complex (SOCAL). Details of these additional case studies and the challenges they present for estimating the effects of sonar exposure are described in Appendix B.

[Fig. 1 about here]

2.2. Overview of modelling approach

We model movement probability in and out of a region encompassing a Navy range where sonar exercises take place, and how this probability is influenced by the use of sonar on the range. The goal of the resulting approach is the estimation of the distribution of aggregate exposure and response to sonar across individuals in a population over long time periods (e.g., 1 year). The models presented below are implemented in the `mmre` `R` package; see `https://github.com/cmjt/mmre` and Appendix C for further details and examples.

Our modelling approach consisted of three interconnected steps. First, raw tracking data were filtered for obvious mistakes in animal relocation, identified based on unrealistic horizontal displacement. While subsequent models can accommodate for uncertainty in satellite-derived locations of the animals, aberrant observations can negatively affect model performance (Patterson et al., 2010). In brief, we filtered recorded Argos locations using the `R` package `argosfilter` (Freitas, 2012), so that highly unlikely observations (i.e., those implying a horizontal displacement greater than 15 m/s) were removed. Post filtering, individuals with fewer than fifty observations were excluded from the analysis.

Second, filtered tracks were corrected for Argos location uncertainty using a continuous-time correlated random walk state-space model, which returned estimated tracks based on the underlying movement model (Section 2.3).

Finally, estimated tracks were analyzed using a continuous-time Markov model that quantified the transition rates across range boundaries and the effect of exposure to sonar disturbance on animal movement patterns, see Section 2.4. A full propagation of the uncertainty associated with estimated tracks to the results of the Markov model was achieved using multiple imputation from the correlated random walk model, see Section 2.6.

2.3. Continuous-time correlated random walk

Due to the uncertainty associated with Argos locations, individual tracks were estimated using the continuous-time correlated random walk model

(CTCRW) described in Johnson et al. (2008) and Albertsen et al. (2015) using the `R` package `argosTrack` (Albertsen, 2017).

In brief, the CTCRW model is a state space model (SSM) with measurement equation given by

$$y_{ct} = \mu_{ct} + \epsilon_{ct}$$

where y_{ct} is the cth coordinate ($c = 1, 2$) of the observed location of an animal at time t ($t = 1, 2, ..., n$) with measurement error term ϵ_{ct}. As in Albertsen et al. (2015) the joint distribution of ϵ_{1t} and ϵ_{2t} is a bivariate t-distribution. The term μ_{ct} is then the "true" cth coordinate location of the animal at time t. This location process, μ_{ct}, is obtained by integrating over the assumed instantaneous velocity of the animal at time t. This velocity is assumed to follow an Orstein-Uhlenbeck (OU) process (see Albertsen et al. (2015) for further details).

2.4. Discrete-space continuous-time Markov model

A continuous-time Markov model describes how an individual transitions between states in continuous time. Given that an individual is in state $S(t)$ at time t, the transition intensity, $q_{rs}(t, z(t))$, represents the immediate risk of moving from one state r to another state s, and may be dependent on the time t of the process as well as some time-varying covariate $z(t)$. These transition intensities can be written as

$$q_{rs}(t, z(t)) = \lim_{\delta t \to 0} \mathbb{P}(S(t + \delta t) = s | S(t) = r)/\delta t$$

and form a square matrix $\mathbf{Q}$ with elements q_{rs} where $q_{rr} = -\Sigma_{s \neq r} q_{rs}$ (i.e., the rows of $\mathbf{Q}$ sum to zero) and $q_{rs} \geq 0$ for $r \neq s$. We consider only two states (i.e., $r, s = \{1, 2\}$) where state 1 = off-range (i.e., outside the area used by the Navy for military operations) and state 2 = on-range (i.e., inside the area of interest, see Fig. 1), so that

$$\mathbf{Q} = \begin{bmatrix} q_{11} & q_{12} \\ q_{21} & q_{22} \end{bmatrix} \quad \text{where } q_{rr} = -q_{rs}, \quad \text{for } r \neq s \tag{1}$$

2.4.1. Including individual-level random effects on the transition rates

We use the `R` package `msm` (which fits continuous-time Markov models (Jackson, 2011)) as a benchmark for the model given by Equation (1), see Appendix A. In an extension to the functionality of the `msm` package, we allow for individual-level variation in our model by considering each off-diagonal elements of $\mathbf{Q}$ (i.e., $q_{k,rs}$ where, for individual k, $r \neq s$) to be given by

$$\log(q_{k,rs}) = \beta_{0,rs} + u_{k,rs}. \tag{2}$$

Here, each $\boldsymbol{u}_k = \{u_{k,rs}, u_{k,sr}\}$ follows a zero-mean bivariate Gaussian distribution (between states r and s) with 2×2 variance covariance matrix $\text{diag}(\sigma_u^2, \sigma_u^2)$.

2.4.2. Including exposure information

We extend Equation 2 to model the effect of exposure to sonar on the transition rate, and let

$$\log(q_{k,rs}(\mathbf{z}_k(t))) = (\beta_{0,rs} + u_{k,rs}) + \beta_{1,rs}\exp(-\beta_{2,rs}\mathbf{z}_k(t)), \tag{3}$$

where

$$\mathbf{z}_k(t) \begin{cases} = 0 & \text{during exposure} \\ \geq 0 & \text{otherwise} \end{cases}$$

is the number of days since an individual was exposed to a sonar event.

Here, $\beta_{1,rs}$ represents the change in transition rate, on the log scale, during exposure (i.e., $\mathbf{z}_k(t) = 0$, and $\exp(-\beta_{2,rs}\mathbf{z}_k(t)) = 1$). We constrain $\beta_{2,rs} \geq 0$ $\forall\, r \neq s$; by doing so, as the number of days since an individual was exposed to sonar, $\mathbf{z}_k(t)$, increases, transition rates decay exponentially towards their baseline values, $\beta_{0,rs}$ (on the log scale).

2.4.3. Likelihood

The transition probability matrix is given by $\mathbf{P}(t)$, where each element $p_{rs}(t)$ is the probability that, given an individual is currently in state r, they will be in state s at time t in the future. This transition probability matrix can be calculated by taking the matrix exponential of the scaled transition intensity matrix as follows:

$$\mathbf{P}(t) = \mathrm{Exp}(t\mathbf{Q}). \tag{4}$$

The likelihood, $L(\mathbf{Q})$, is calculated as the product, over all individuals and all transitions, of the probabilities that individual k is in state $S(t_{j+1})$ at time t_{j+1} given they were in state $S(t_j)$ at time t_j, evaluated at time $t_{j+1} - t_j$ (for $j = 1, ..., n_k$):

$$L(\boldsymbol{Q}) = \prod_{k,j} L_{k,j} = \prod_{k,j} p_{S(t_j)S(t_{j+1})}(t_{j+1} - t_j). \tag{5}$$

Parameter estimates are obtained via minimisation of the negative log-likelihood, $-\log(L(\mathbf{Q}))$.

2.5. Simulation

To assess the performance of the proposed model, we used the estimated parameter values from the fitted model (Equation 3) to simulate new datasets. Specifically, we simulated the states of individuals at each observed time using the fitted transition probabilities. This was done 500 times for each individual. We refitted the model to the 500 simulated datasets, and calculated root mean squared errors for each parameter, as well as the % errors for $\beta_{1,12}$, $\beta_{1,21}$, $\beta_{2,12}$, and $\beta_{2,21}$ (that is, the parameters relating to the sonar effect).

2.6. Multiple imputation

We used a multiple imputation procedure to show how the uncertainty associated with the Argos tracks could be propagated to the Markov model (McClintock and Michelot, 2018). For each of the seven individuals, a total of 100 tracks were simulated using the estimated bivariate t-distribution of measurement error from the CTCRW model, fitted to the Argos tracks, see Section 2.3.

We fitted the model given by Equation (3) to the 100 simulated datasets (each containing one potential track per individual), and averaged the estimated parameter values across the fitted models to obtain point estimates and associated standard errors.

2.7. Goodness of fit

To assess the goodness of fit of the Markov model, we took a similar approach to that detailed in Aguirre-Hernández and Farewell (2002). Specifically, we partitioned the observations from each individual by time and covariate value (time since exposure), and compared the observed number of transitions, o, to the number of transitions expected under the fitted model, e. Bins were created by splitting the data into quantiles, [0%–25%), [25%–50%), [50%–75%), and [75%–100%], based on the observation times and the covariate values (using the estimated transition rates as recommended by Aguirre-Hernández and Farewell (2002)). The expected number of transitions in each cell of the resulting confusion matrix (i.e., in each time and

covariate bin) were calculated as the sum of the estimated probabilities classified in that category.

We carried out a Pearson-type goodness-of-fit test similar to that proposed by Aguirre-Hernández and Farewell (2002) using the test statistic $T = \Sigma_{u,h,w} \frac{(o_{uhw} - e_{uhw})^2}{e_{uhw}}$, where u represented the number of levels defined by the quantiles of the observation times, h represented the groupings due to the covariate, and w was the individual whale. We assumed a chi-squared distribution for this test statistic and used both a liberal and a conservative number of degrees of freedom; these were calculated as 1) the minimum number of independent bins ($7 \times 4 \times 3 \times 2 = w \times u \times h \times n_{states}$), and 2) the minimum number of independent bins minus the number of estimated parameters, $n_p = 20$, respectively.

3. Results

Following the first two steps of our analytical approach, we obtained estimates of the corrected tracks for the seven Blainville's beaked whales tagged on AUTEC (Fig. 1). The discrete-space continuous-time Markov model was then used to estimate the transition rates across the AUTEC range boundaries (Table 1). Differences in baseline transition rates among individuals were captured by the inclusion of individual-level random effects (Equation (2), see Section 2.4.1); Figs 3 and 2 show that there was noteworthy variation among whales.

[Fig. 2 about here]

Using the model given by Equation (3), we detected a change in transition rates following exposure to sonar activities (Table 1). The AIC suggests that this effect should be retained in the model. The estimated $\hat{\boldsymbol{\beta}}_1 = \{\hat{\beta}_{1,12}, \hat{\beta}_{1,21}\}^T$ parameters represent the effect on the log rate of transition off–on and on–off the range, respectively, during the time an individual was exposed to sonar. During exposure (i.e., $\mathbf{z}(t) = 0$ in Equation (3)), transitions onto the range (off–on) decreased ($\hat{\beta}_{1,12} = -0.60$) and transitions off the range (on–off) increased ($\hat{\beta}_{1,21} = 1.75$). The increase in on–off transitions during sonar exposure is illustrated in Fig. 3, where sonar activity is indicated by vertical grey lines.

The $\hat{\boldsymbol{\beta}}_2 = \{\hat{\beta}_{2,12}, \hat{\beta}_{2,21}\}^T = \{0.78, 0.85\}$ parameters describe the lessening effect of sonar exposure on the transition rates after the termination of sonar activity on the range (i.e., the exponential decay to the baseline transition rates off–on range and on–off range, respectively). Figs 3 and 2 illustrate this exponential decay for each individual; the effect of sonar exposure on transition rates was estimated to end approximately 3 days after the activity ended (i.e., when transition probabilities returned to their baseline values). Fig. A.2 in the Appendix shows the estimated individual level random effects.

[Table 1 about here]

[Fig. 3 about here]

Refitting the Markov model to 500 simulated datasets, generated using the estimates in Table 1, suggested that the model was able to retrieve the values of the parameters with limited bias. Root mean squared errors for each parameter are given in Table A.4, while the % errors for the parameters relating to sonar effect are shown in Fig. A.3.

The multiple imputation procedure allowed us to successfully propagate the uncertainty in the telemetry tracks across all modelling steps. A subset of 20 simulated tracks obtained using the parameter values from the fitted CTCRW model are shown in Fig. A.1 for 3 individuals. Uncertainty in the exact locations of the individuals had little effect on the estimated transition rates shown in Section 3, as suggested by the parameter values averaged across the 100 fitted models (Fig. A.3 and Table 2).

The comparison of observed transitions $o.$ (aggregated into bins based on quantiles of the observation times and covariate value; see Section 2.7) with those expected, $e.$, for each individual w suggested that the goodness-of-fit of the Markov model was satisfactory (Fig. A.3 plot c). The Pearson-type test returned a test statistic $T = 168.44$; under $T \sim \chi^2_{148}$ $\mathbb{P}(T > 168.44) = 0.476$ and under $T \sim \chi^2_{168}$ $\mathbb{P}(T > 168.44) = 0.120$, i.e., we have no evidence to

suggest that observed frequencies in each cell are significantly different from those estimated by our model.

4. Discussion

We developed a modelling approach that quantifies the rates at which animals move across the boundaries of a discrete area of interest. The model can therefore be used to describe patterns of attendance to that area. Individual differences in movement and ranging behaviour, which may lead to heterogeneity in area use, are explicitly evaluated. By fitting a movement model to the raw telemetry tracks, uncertainty in animal relocations can also be accounted for. Moreover, because the Markovian component is formulated in continuous time, the approach does not require observations regularly sampled in time. These features are important, because wildlife telemetry often involves irregular relocations with substantial measurement error (Patterson et al., 2017). Crucially, the method we propose can be used to investigate the repulsive (or attractive) effect of a given stressor or activity, operating either within or outside the target area and affecting the propensity of an individual to cross the boundaries in either direction. Our simulation exercise showed that the model performs well at estimating transition rates and any change associated with exposure to disturbance.

We used a CTCRW model to correct for uncertainty in animal relocations (Albertsen et al., 2015; Johnson et al., 2008). Alternative movement models could be fitted, depending on the sampling frequency and degree of mea-

surement error in the telemetry data (Patterson et al., 2017). Irrespective of the underlying movement model, we showed how a multiple imputation procedure can be used to propagate any such uncertainty (McClintock and Michelot, 2018). Our results suggest that relocation error does not alter the conclusions here, probably due to the size of the target area in relation to the estimated uncertainty.

In this study, we applied the proposed approach to a specific management problem: the assessment of the effects of exposure to military sonar operations within navy ranges on the movement behaviour of cetaceans, and the resulting attendance of individuals to these range areas (Bernaldo de Quirós et al., 2019; Southall et al., 2016; Nowacek et al., 2007). When fitted to tracking data from Blainville's beaked whales tagged on or near the AUTEC US Navy range in the Bahamas, the model detected a change in the animals' movements following exposure: specifically, individual whales that were on the range at the time of exposure showed an increased tendency of leaving the range, while individuals that were outside the range area had a lower propensity to move onto the range, overall indicating an avoidance response to sonar. This effect was found to last for approximately three days after the end of the exposure, during which the transition rates progressively returned to their baseline values.

The implications of these results are twofold. First, they contribute to the increasing body of evidence suggesting that military sonar operations can cause changes in the behaviour of exposed beaked whales (Harris et al.,

2018; Falcone et al., 2017; Tyack et al., 2011; Bernaldo de Quirós et al., 2019; Wensveen et al., 2019; De Ruiter et al., 2013; Stimpert et al., 2014). Dedicated experimental studies, as well as observational studies, have shown that these species modify their horizontal movement and diving pattern when exposed to simulated or real sonar in this and other areas. In particular, passive acoustic monitoring of whale echolocation clicks has previously suggested that Blainville's beaked whale detections decline within the range area in AUTEC during sonar exercises, returning to baseline levels after approximately three days (Tyack et al., 2011; McCarthy et al., 2011). Using the same telemetry data we have analysed here, and focusing only on the effects of large-scale exercises (Submarine Command Courses), a recent study has provided further indication that this indeed corresponds to animals moving out of the range, rather than cessation of acoustic vocalisations (Joyce et al., 2019). With the proposed approach, we were able to quantify this tendency in terms of individual transition rates, and show that avoidance emerges in response to all sonar exercises occurring on the range. It has been suggested that human disturbance is perceived by wildlife as a form of predation risk, and, as such, can elicit comparable reactions, for example attempts to move away from the stressor (Frid and Dill, 2002). A similar response could also arise indirectly if beaked whale prey became less available due to sonar activity (e.g., through displacement or changes in patch characteristics). We detected this behavioural change despite the regular exposure of this population to sonar disturbance in the range area, which poses interesting questions

on the role of tolerance, habituation, and availability of alternative habitat (Harris et al., 2018).

Secondly, our model can support the assessment of the total duration and intensity of exposure of individuals to a stressor (that is, their aggregate exposure) (Pirotta et al., 2018a). In particular, the model determines the presence of an individual in the area where the stressor operates, which can then be combined with approaches that simulate fine-scale movements. To date, these simulations have incurred the problem that, as time progresses, simulated individuals tend to drift away from the target area (Frankel et al., 2002; Donovan et al., 2017; Houser, 2006), leading to unrealistic movement patterns and thus compromising the ability to estimate aggregate exposure over time scales that are biologically relevant (e.g. one year). The results of our model can be used to simulate realistic occurrence in the area where an individual is potentially exposed, and ignore the behaviour when outside such area (although this will require adjusting the range boundaries to account for noise propagation and potential exposure outside the instrumented area (Joyce et al., 2019)). In some cases (e.g., when animals do not show high residency levels), this will also allow saving substantial computation time, which is important when many scenarios of disturbance need to be simulated efficiently for large populations.

Model results highlighted differences among individuals in transition rates and presence on the range, which will result in heterogeneous levels of aggregate exposure within the population (Pirotta et al., 2018b; Jones et al., 2017;

Merchant et al., 2018). Differences among individuals could be explained by sex, age, life history stage, body condition or social preferences. This information, when available, could readily be incorporated into the model as fixed effects on the transition rates. These differences are relevant because long-term effects on individual vital rates tend to emerge from the chronic disruption of activity budget and the impaired ability to acquire energy (Pirotta et al., 2018a). Therefore, characterising variation in exposure and identifying the proportion of the population with high exposure level will ultimately contribute to the assessment of the population-level consequences of disturbance resulting from human activities, an important target for many regulatory frameworks and a requirement for the US Navy on their ranges (Pirotta et al., 2018a; National Research Council, 2005; National Academies, 2017).

The application of the modelling approach to other case studies in different US Navy ranges demonstrates some of the outstanding challenges associated with this analysis (see Appendix B). Particularly, the model might not be appropriate in situations where the animals rarely leave the target area, as shown for rough-toothed dolphins *Steno bredanensis* in Hawaii (Baird et al., 2019; Baird, 2016) and Cuvier's beaked whales *Ziphius cavirostris* in southern California (Falcone et al., 2017). In the latter case, the short time-scale of documented behavioural responses (Falcone et al., 2017) compared to the resolution of the telemetry data further complicates the use of the model. In that region, the model could be more appropriate for fin whales *Balaenoptera*

physalus, which regularly transits in and out of the area where sonar activities operate (Scales et al., 2017), but uncertainty on the boundaries of such area also presents an issue. Access to reliable information on the spatial and temporal patterns of sonar occurrence is critical for the proposed approach. The comparison of the SPORTS database with acoustic recordings on Navy ranges has shown that the database is prone to transcription errors and incomplete records (Falcone et al., 2017), which have likely contributed to the problems encountered when fitting the model to the additional case studies.

Beyond the effects of disturbance resulting from military sonar operations on cetacean species, our approach can be used to quantify the exposure to any activity that occurs within a discrete area and has either an attractive or a repulsive effect on exposed animals. Potential examples include attendance of marine predators to fish farms (Callier et al., 2018), changes in use of windfarm areas by birds (Pearce-Higgins et al., 2009), attractions to supplemental feeding sites for a range of species (Corcoran et al., 2013), temporal variation in the use of refuges as a function of anthropogenic risk in terrestrial ungulates (Visscher et al., 2017), or elephant occurrence in areas with differential human-associated mortality risk (Graham et al., 2009). More generally, it is often valuable to assess the probability of occurrence within predefined regions, e.g. to evaluate the effectiveness of the boundaries of a protected area for covering the occupancy of a sufficiently large proportion of a population (Cabeza et al., 2004; Lea et al., 2016; Licona et al., 2011), a common application of telemetry data (Hays et al., 2019). The transition rates estimated

in our model would inform decisions regarding such boundaries.

The approach can be easily extended to model additional states, that is, additional discrete areas where individual patterns of occurrence are of interest. For example, the model could be used to estimate the connectivity among multiple protected areas, or the degree of usage of distinct portions of a population's range, e.g. (Webster et al., 2002; Espinoza et al., 2015). The effect of other covariates (e.g. environmental characteristics) on the transitions among areas could be included to elucidate the ecological or anthropogenic processes influencing these movement patterns.

In conclusion, we introduced a versatile method to monitor animals' attendance to discrete areas in continuous time, and assess the effects of stressors or attractors on the transition rates across these predefined boundaries. We used the method to quantify the effect of sonar on the occurrence of a cetacean species on a US Navy range, and found changes in the propensity of moving in and out of this area as a result of exposure. These results will help to assess the aggregate exposure of individuals and any resulting population-level consequences, a legal requirement for the US Navy in the range area. However, we anticipate the model could have wide applications in both applied and fundamental ecological studies that use telemetry data to characterise animal movements.

5. Authors' contributions

CJT, EP and LT conceived the ideas and developed the methodology; RWB, JD, EF, TJ, GS, and ST collected and obtained permissions for use of the data. CJT and EP analysed the data and led the writing of the manuscript. All authors contributed critically to the drafts and gave final approval for publication.

6. Acknowledgements

This study was supported by Office of Naval Research (ONR) grant N00014-16-1-2858: "PCoD+: Developing widely-applicable models of the population consequences of disturbance". We thank Ruth Joy, Rob Schick, John Harwood, Cormac Booth, Leslie New, Dan Costa and Lisa Schwarz for useful discussions during the development of the modelling approach.

Tagging in AUTEC was conducted under Bahamas Marine Mammal Research Permit #12A. issued by the Government of the Bahamas to the Bahamas Marine Mammal Research Organisation (BMMRO) under the regulatory framework of the Bahamas Marine Mammal Protection Act (2005). Methods of deployment, tag types, and sample sizes were preapproved by BMMRO's Institutional Animal Care and Use Committee (IACUC) and by the US Department of the Navy, Bureau of Medicine and Surgery (BUMED) Veterinary Affairs Office. Protocols were reviewed annually by BMMRO's IACUC throughout the duration of the study.

Funding support for tagging was provided by the US Navy's Office of Naval Research and Living Marine Resources program, the Chief of Naval Operations' Energy and Environmental Readiness Division and the NOAA Fisheries Ocean Acoustics Program (See Joyce et al. (2019) for details).

The authors wish to acknowledge the use of New Zealand eScience Infrastructure (NeSI) high performance computing facilities, consulting support and/or training services as part of this research. New Zealand's national facilities are provided by NeSI and funded jointly by NeSI's collaborator institutions and through the Ministry of Business, Innovation & Employment's Research Infrastructure programme. URL `https://www.nesi.org.nz`.

7. Data availability statement

Due to security reasons, information on the location and timing of U.S. military sonar exercises cannot be released publicly. However, simulated sonar times are included in the examples of the `mmre` `R` package (see `https://github.com/cmjt/mmre` and Appendix C). Whale tracking data will be uploaded on the Dryad Digital Repository upon acceptance.

References

Aguirre-Hernández, R. and Farewell, V. (2002). A Pearson-type goodness-of-fit test for stationary and time-continuous Markov regression models. *Statistics in medicine*, 21(13):1899–1911.

Albertsen, C. M. (2017). *argosTrack: Fit Movement Models to Argos Data for Marine Animals*. R package version 1.1.0.

Albertsen, C. M., Whoriskey, K., Yurkowski, D., Nielsen, A., and Mills, J. (2015). Fast fitting of non-Gaussian state-space models to animal movement data via Template Model Builder. *Ecology*, 96(10):2598–2604.

Baird, R. (2016). *The lives of Hawai'i's dolphins and whales: natural history and conservation*. University of Hawai'i Press, Honolulu, Hawai'i.

Baird, R., Webster, D., Jarvis, S., Henderson, E., Watwood, S., Mahaffy, S., Guenther, B., Lerma, C., Cornforth, A., Vanderzee, A., and Anderson, D. (2019). Odontocete studies on the Pacific Missile Range Facility in August 2018: satellite-tagging, photo-identification, and passive acoustic monitoring. Prepared for Commander, Pacific Fleet, under Contract No. N62470-15-D-8006 Task Order 6274218F0107 issued to HDR Inc., Honolulu, HI.

Bernaldo de Quirós, Y., Fernandez, A., Baird, R., Brownell Jr, R., Aguilar de Soto, N., Allen, D., Arbelo, M., Arregui, M., Costidis, A., Fahlman, A., et al. (2019). Advances in research on the impacts of anti-submarine sonar

561 on beaked whales. *Proceedings of the Royal Society of London. Series B:*
562 *Biological Sciences*, 286(1895):20182533.

563 Cabeza, M., Araújo, M. B., Wilson, R. J., Thomas, C. D., Cowley, M. J. R.,
564 and Moilanen, A. (2004). Combining probabilities of occurrence with spa-
565 tial reserve design. *Journal of Applied Ecology*, 41(2):252–262.

566 Callier, M. D., Byron, C. J., Bengtson, D. A., Cranford, P. J., Cross, S. F.,
567 Focken, U., Jansen, H. M., Kamermans, P., Kiessling, A., Landry, T., et al.
568 (2018). Attraction and repulsion of mobile wild organisms to finfish and
569 shellfish aquaculture: a review. *Reviews in Aquaculture*, 10(4):924–949.

570 Corcoran, M. J., Wetherbee, B. M., Shivji, M. S., Potenski, M. D., Chapman,
571 D. D., and Harvey, G. M. (2013). Supplemental feeding for ecotourism
572 reverses diel activity and alters movement patterns and spatial distribution
573 of the southern stingray, dasyatis americana. *PLoS One*, 8(3):e59235.

574 Costa, D. P., Robinson, P. W., Arnould, J. P., Harrison, A. L., Simmons,
575 S. E., Hassrick, J. L., Hoskins, A. J., Kirkman, S. P., Oosthuizen, H.,
576 Villegas-Amtmann, S., and Crocker, D. E. (2010). Accuracy of ARGOS
577 locations of pinnipeds at-sea estimated using fastloc GPS. *PLoS One*, 5(1).

578 De Ruiter, S. L., Southall, B. L., Calambokidis, J., Zimmer, W. M.,
579 Sadykova, D., Falcone, E. A., Friedlaender, A. S., Joseph, J. E., Moretti,
580 D., Schorr, G. S., et al. (2013). First direct measurements of behavioural

responses by cuvier's beaked whales to mid-frequency active sonar. *Biology Letters*, 9(4):20130223.

Díaz, S., Settele, J., Brondízio, E., Ngo, H., Guèze, M., Agard, J., Arneth, A., Balvanera, P., Brauman, K., Butchart, S., et al. (2019). Summary for policymakers of the global assessment report on biodiversity and ecosystem services of the intergovernmental science-policy platform on biodiversity and ecosystem services.

Donovan, C. R., Harris, C. M., Milazzo, L., Harwood, J., Marshall, L., and Williams, R. (2017). A simulation approach to assessing environmental risk of sound exposure to marine mammals. *Ecology and Evolution*, 7(7):2101–2111.

Espinoza, M., Lédée, E. J. I., Simpfendorfer, C. A., Tobin, A. J., and Heupel, M. R. (2015). Contrasting movements and connectivity of reef-associated sharks using acoustic telemetry: implications for management. *Ecological Applications*, 25(8):2101–2118.

Falcone, E. A., Schorr, G. S., Watwood, S. L., De Ruiter, S. L., Zerbini, A. N., Andrews, R. D., Morrissey, R. P., and Moretti, D. J. (2017). Diving behaviour of Cuvier's beaked whales exposed to two types of military sonar. *Royal Society Open Science*, 4:170629.

Frankel, A. S., Ellison, W. T., and Buchanan, J. (2002). Application of the

601 Acoustic Integration Model (AIM) to predict and minimize environmental
602 impacts. *IEEE Journal of Oceanic Engineering*, 3:1438–1443.

603 Freitas, C. (2012). *argosfilter: Argos locations filter*. R package version 0.63.

604 Frid, A. and Dill, L. (2002). Human-caused disturbance stimuli as a form of
605 predation risk. *Conservation Ecology*, 6(1):11.

606 Graham, M. D., Douglas-Hamilton, I., Adams, W. M., and Lee, P. C. (2009).
607 The movement of african elephants in a human-dominated land-use mosaic.
608 *Animal Conservation*, 12(5):445–455.

609 Halpern, B. S., Walbridge, S., Selkoe, K. A., Kappel, C. V., Micheli, F.,
610 D'Agrosa, C., Bruno, J. F., Casey, K. S., Ebert, C., Fox, H. E., Fujita,
611 R., Heinemann, D., Lenihan, H. S., Madin, E. M. P., Perry, M. T., Selig,
612 E. R., Spalding, M., Steneck, R., and Watson, R. (2008). A global map of
613 human impact on marine ecosystems. *Science*, 319(5865):948–52.

614 Harris, C. M., Thomas, L., Falcone, E. A., Hildebrand, J., Houser, D., Kvad-
615 sheim, P. H., Lam, F.-P. A., Miller, P. J. O., Moretti, D. J., Read, A. J.,
616 Slabbekoorn, H., Southall, B. L., Tyack, P. L., Wartzok, D., and Janik,
617 V. M. (2018). Marine mammals and sonar: dose-response studies, the
618 risk-disturbance hypothesis and the role of exposure context. *Journal of*
619 *Applied Ecology*, 55(1):396–404.

620 Hays, G. C., Bailey, H., Bograd, S. J., Bowen, W. D., Campagna, C.,
621 Carmichael, R. H., Casale, P., Chiaradia, A., Costa, D. P., Cuevas, E.,

et al. (2019). Translating marine animal tracking data into conservation policy and management. *Trends in Ecology & Evolution*, 34(5):459 – 473.

Houser, D. S. (2006). A method for modeling marine mammal movement and behavior for environmental impact assessment. *IEEE Journal of Oceanic Engineering*, 31(1):76–81.

Jackson, C. H. (2011). Multi-State Models for Panel Data: The msm Package for R. *Journal of Statistical Software*, 38(8):1–29.

Johnson, D. S., London, J. M., Lea, M.-A., and Durban, J. W. (2008). Continuous-time correlated random walk model for animal telemetry data. *Ecology*, 89(5):1208–1215.

Jones, E. L., Hastie, G. D., Smout, S., Onoufriou, J., Merchant, N. D., Brookes, K. L., and Thompson, D. (2017). Seals and shipping: quantifying population risk and individual exposure to vessel noise. *Journal of Applied Ecology*, 54(6):1930–1940.

Joyce, T. W., Durban, J. W., Claridge, D. E., Dunn, C. A., Hickmott, L. S., Fearnbach, H., Dolan, K., and Moretti, D. (2019). Behavioral responses of satellite tracked blainville's beaked whales (*Mesoplodon densirostris*) to mid-frequency active sonar. *Marine Mammal Science*, 0(0).

Lea, J. S. E., Humphries, N. E., von Brandis, R. G., Clarke, C. R., and Sims, D. W. (2016). Acoustic telemetry and network analysis reveal the space use of multiple reef predators and enhance marine protected area design.

643 *Proceedings of the Royal Society of London. Series B: Biological Sciences*,
644 283(1834):20160717.

645 Licona, M., McCleery, R., Collier, B., Brightsmith, D. J., and Lopez, R.
646 (2011). Using ungulate occurrence to evaluate community-based conserva-
647 tion within a biosphere reserve model. *Animal Conservation*, 14(2):206–
648 214.

649 Lopez, R., Malardé, J.-P., Royer, F., and Gaspar, P. (2013). Improving argos
650 doppler location using multiple-model kalman filtering. *IEEE Transactions*
651 *on Geoscience and Remote Sensing*, 52(8):4744–4755.

652 McCarthy, E., Moretti, D., Thomas, L., DiMarzio, N., Morrissey, R., Jarvis,
653 S., Ward, J., Izzi, A., and Dilley, A. (2011). Changes in spatial and tem-
654 poral distribution and vocal behavior of blainville's beaked whales (meso-
655 plodon densirostris) during multiship exercises with mid-frequency sonar.
656 *Marine Mammal Science*, 27(3):E206–E226.

657 McClintock, B. T., London, J. M., Cameron, M. F., and Boveng, P. L. (2015).
658 Modelling animal movement using the Argos satellite telemetry location
659 error ellipse. *Methods in Ecology and Evolution*, 6(3):266–277.

660 McClintock, B. T. and Michelot, T. (2018). momentuhmm: R package for
661 generalized hidden markov models of animal movement. *Methods in Ecol-*
662 *ogy and Evolution*, 9(6):1518–1530.

Merchant, N. D., Faulkner, R. C., and Martinez, R. (2018). Marine noise budgets in practice. *Conservation Letters*, 11(3):e12420.

Montgomery, J. C. and Radford, C. A. (2017). Marine bioacoustics. *Current Biology*, 27(11):R502–R507.

Moretti, D., Thomas, L., Marques, T., Harwood, J., Dilley, A., Neales, B., Shaffer, J., McCarthy, E., New, L., Jarvis, S., and Morrissey, R. (2014). A risk function for behavioral disruption of Blainville's beaked whales (*Mesoplodon densirostris*) from mid-frequency active sonar. *PloS One*, 9(1):e85064.

National Academies (2017). *Approaches to understanding the cumulative effects of stressors on marine mammals*. The National Academies Press, Washington, DC.

National Research Council (2005). *Marine mammal populations and ocean noise: determining when noise causes biologically significant effects*. The National Academies Press, Washington, DC.

Nowacek, D. P., Thorne, L. H., Johnston, D. W., and Tyack, P. L. (2007). Responses of cetaceans to anthropogenic noise. *Mammal Review*, 37(2):81–115.

Patterson, T. A., McConnell, B. J., Fedak, M. A., Bravington, M. V., and Hindell, M. A. (2010). Using gps data to evaluate the accuracy of

683 state–space methods for correction of argos satellite telemetry error. *Ecol-*
684 *ogy*, 91(1):273–285.

685 Patterson, T. A., Parton, A., Langrock, R., Blackwell, P. G., Thomas, L.,
686 and King, R. (2017). Statistical modelling of individual animal movement:
687 an overview of key methods and a discussion of practical challenges. *AStA*
688 *Advances in Statistical Analysis*, 101(4):399–438.

689 Pearce-Higgins, J. W., Stephen, L., Langston, R. H., Bainbridge, I. P., and
690 Bullman, R. (2009). The distribution of breeding birds around upland
691 wind farms. *Journal of Applied Ecology*, 46(6):1323–1331.

692 Pirotta, E., Booth, C. G., Costa, D. P., Fleishman, E., Kraus, S. D., Lusseau,
693 D., Moretti, D., New, L. F., Schick, R. S., Schwarz, L. K., Simmons,
694 S. E., Thomas, L., Tyack, P. L., Weise, M. J., Wells, R. S., and Harwood,
695 J. (2018a). Understanding the population consequences of disturbance.
696 *Ecology and Evolution*, 8(19):9934–9946.

697 Pirotta, E., New, L., and Marcoux, M. (2018b). Modelling beluga habitat
698 use and baseline exposure to shipping traffic to design effective protec-
699 tion against prospective industrialization in the Canadian Arctic. *Aquatic*
700 *Conservation: Marine and Freshwater Ecosystems*, 28(3):713–722.

701 Popper, A. N. and Hawkins, A. (2016). *The effects of noise on aquatic life*
702 *II*. Springer.

Sanderson, E. W., Jaiteh, M., Levy, M. A., Redford, K. H., Wannebo, A. V., and Woolmer, G. (2002). The human footprint and the last of the wild: the human footprint is a global map of human influence on the land surface, which suggests that human beings are stewards of nature, whether we like it or not. *BioScience*, 52(10):891–904.

Scales, K. L., Schorr, G. S., Hazen, E. L., Bograd, S. J., Miller, P. I., Andrews, R. D., Zerbini, A. N., and Falcone, E. A. (2017). Should I stay or should I go? Modelling year-round habitat suitability and drivers of residency for fin whales in the California Current. *Diversity and Distributions*, 23(10):1204–1215.

Southall, B. L., Nowacek, D. P., Miller, P. J., and Tyack, P. L. (2016). Experimental field studies to measure behavioral responses of cetaceans to sonar. *Endangered Species Research*, 31(1):293–315.

Stimpert, A. K., De Ruiter, S. L., Southall, B. L., Moretti, D. J., Falcone, E. A., Goldbogen, J. A., Friedlaender, A., Schorr, G. S., and Calambokidis, J. (2014). Acoustic and foraging behavior of a Baird's beaked whale, *Berardius bairdii*, exposed to simulated sonar. *Scientific Reports*, 4:7031.

Tyack, P. L., Zimmer, W. M. X., Moretti, D., Southall, B. L., Claridge, D. E., Durban, J. W., Clark, C. W., D'Amico, A., DiMarzio, N., Jarvis, S., McCarthy, E., Morrissey, R., Ward, J., and Boyd, I. L. (2011). Beaked whales respond to simulated and actual navy sonar. *PLoS ONE*, 6(3):e17009–.

U.S. Department of the Navy (2018). Quantifying acoustic impacts on marine mammals and sea turtles: methods and analytical approach for phase iii training and testing. nuwc division newport, space and naval warfare systems center pacific, g2 software systems, and the national marine mammal foundation. newport, ri: Naval undersea warfare center. Technical report.

Visscher, D. R., Macleod, I., Vujnovic, K., Vujnovic, D., and Dewitt, P. D. (2017). Human risk induced behavioral shifts in refuge use by elk in an agricultural matrix. *Wildlife Society Bulletin*, 41(1):162–169.

Webster, M. S., Marra, P. P., Haig, S. M., Bensch, S., and Holmes, R. T. (2002). Links between worlds: unraveling migratory connectivity. *Trends in Ecology & Evolution*, 17(2):76 – 83.

Wensveen, P. J., Isojunno, S., Hansen, R. R., von Benda-Beckmann, A. M., Kleivane, L., van IJsselmuide, S., Lam, F.-P. A., Kvadsheim, P. H., De Ruiter, S. L., Curé, C., et al. (2019). Northern bottlenose whales in a pristine environment respond strongly to close and distant navy sonar signals. *Proceedings of the Royal Society of London. Series B: Biological Sciences*, 286(1899):20182592.

Figures

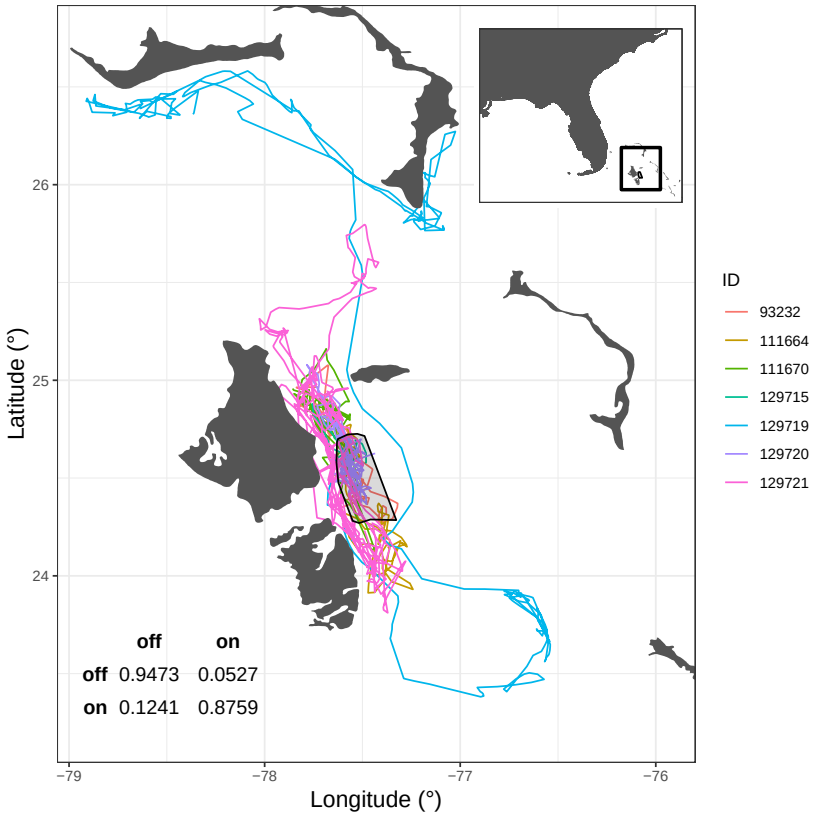

Figure 1: Corrected tracks of seven Blainville's beaked whales *(Mesoplodon densirostris)*—Tag IDs given in legend—at the AUTEC range (shown by the black polygon), Bahamas. Inset table shows the calculated raw transition probability matrix for sequential transitions across AUTEC range boundaries, averaged across individuals. The number of observations estimated as either on- or off-range are show per individual in Table A.2. Inset topright shows the plotted region in relation to Florida, USA.

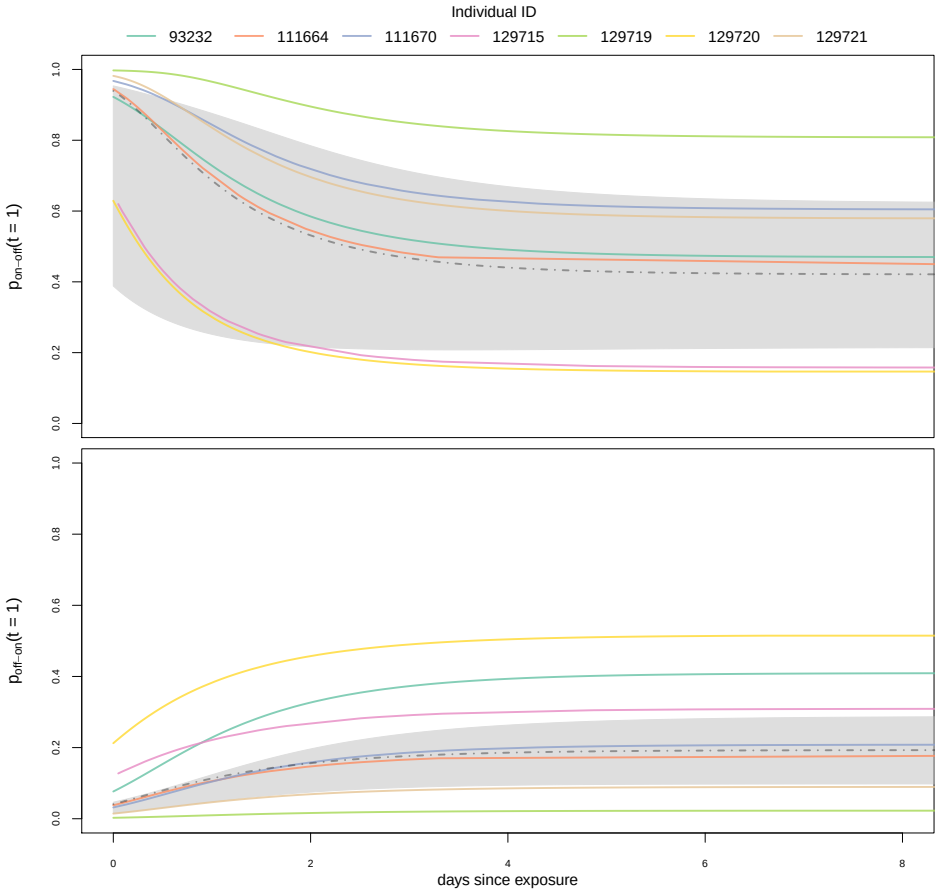

Figure 2: Estimated transition probabilities for each of the seven Blainville's beaked whales as a function of days since exposure to sonar, calculated at one day since tagging ($t = 1$); the corresponding transition rate is given by Equation 3. In each plot, colours indicate different individuals; the top plot shows on–off transition probabilities and the bottom plot shows off—on transition probabilities. The grey shaded areas show the 95% confidence interval around the mean transition probabilities (dashed grey lines) as a function of days since exposure.

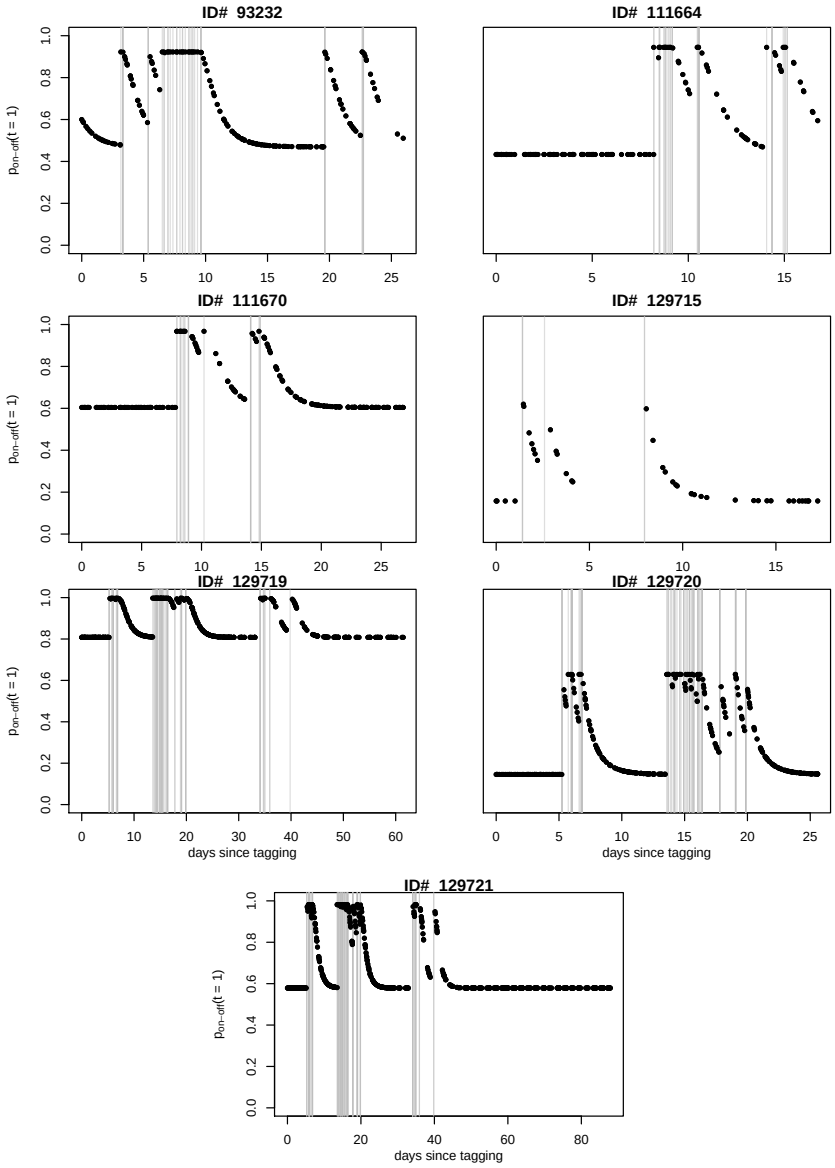

Figure 3: Fitted on–off range transition probabilities, $p_{21}(t = 1)$, for each of the seven Blainville's beaked whales (derived from the corresponding transition rates given by Equation 3). In each plot, the vertical grey lines indicate the time of sonar events; the points represent the time of observed locations (in days) of each individual since tagging. The different horizontal asymptotes in each panel illustrate the differences in baseline transition rates among individuals.

Tables

eq.	$\mathbf{P}(\mathbf{t}=\mathbf{1})^*$	log-likelihood	AIC	$\hat{\boldsymbol{\beta}}_0$	$\hat{\boldsymbol{\beta}}_1$	$\hat{\boldsymbol{\beta}}_2$
1)	$\begin{bmatrix}0.877 & 0.123\\ 0.505 & 0.495\end{bmatrix}$	-257.04	518.08	$\begin{bmatrix}-1.65\ (0.18)\\ -0.23\ (0.16)\end{bmatrix}$	-	-
2)	$\begin{bmatrix}0.858 & 0.142\\ 0.525 & 0.475\end{bmatrix}$	-243.43	492.87	$\begin{bmatrix}-1.45\ (0.40)\\ -0.14\ (0.40)\end{bmatrix}$	-	-
3)	$\begin{bmatrix}0.807 & 0.193\\ 0.421 & 0.579\end{bmatrix}$	-236.26	486.51	$\begin{bmatrix}-1.21\ (0.48)\\ -0.43\ (0.47)\end{bmatrix}$	$\begin{bmatrix}-0.60\ (0.61)\\ 1.75\ (0.56)\end{bmatrix}$	$\begin{bmatrix}0.78\ (1.01)\\ 0.85\ (0.60)\end{bmatrix}$

Table 1: Table of estimated parameters, log-likelihood, and AIC values for each fitted model (standard errors in brackets). The first column indicates the equation number for the corresponding Markov model (see Section 2.3). The baseline transition rates, on the log scale, are given by $\hat{\boldsymbol{\beta}}_0 = \{\hat{\beta}_{0,12}, \hat{\beta}_{0,21}\}^T$. Where applicable, the changes in transition rate during exposure are given by $\hat{\boldsymbol{\beta}}_1 = \{\hat{\beta}_{1,12}, \hat{\beta}_{1,21}\}^T$ and the decay parameters are given by $\hat{\boldsymbol{\beta}}_2 = \{\hat{\beta}_{2,12}, \hat{\beta}_{2,21}\}^T$. Here, * denotes that $\mathbf{P}(\mathbf{t} = \mathbf{1})$ is calculated at the baseline transition rate (i.e., ignoring any other effects, if there are any).

$\mathbf{P}(\mathbf{t}=\mathbf{1})^*$	$\hat{\boldsymbol{\beta}}_0$	$\hat{\boldsymbol{\beta}}_1$	$\hat{\boldsymbol{\beta}}_2$
$\begin{bmatrix} 0.801 & 0.199 \\ 0.416 & 0.584 \end{bmatrix}$	$\begin{bmatrix} -1.18\ (0.01) \\ -0.44\ (0.01) \end{bmatrix}$	$\begin{bmatrix} -0.61\ (0.03) \\ 0.64\ (0.06) \end{bmatrix}$	$\begin{bmatrix} 1.97\ (0.02) \\ 0.98\ (0.02) \end{bmatrix}$

Table 2: Point estimates and standard errors (in brackets) for the parameters in Equation 3 obtained from fitting models to 100 sets of imputed tracks for each of the seven Blainville's beaked whales.